General Disclaimer

One or more of the Following Statements may affect this Document

- This document has been reproduced from the best copy furnished by the organizational source. It is being released in the interest of making available as much information as possible.

- This document may contain data, which exceeds the sheet parameters. It was furnished in this condition by the organizational source and is the best copy available.

- This document may contain tone-on-tone or color graphs, charts and/or pictures, which have been reproduced in black and white.

- This document is paginated as submitted by the original source.

- Portions of this document are not fully legible due to the historical nature of some of the material. However, it is the best reproduction available from the original submission.

X-692-77-213
PREPRINT

TMX 71400

SOURCES OF MAGNETIC FIELDS IN RECURRENT INTERPLANETARY STREAMS

L. F. BURLAGA
K. W. BEHANNON
S. F. HANSEN
G. W. PNEUMAN
W. C. FELDMAN

SEPTEMBER 1977

GSFC — GODDARD SPACE FLIGHT CENTER —
GREENBELT, MARYLAND

SOURCES OF MAGNETIC FIELDS IN RECURRENT INTERPLANETARY STREAMS

L. F. Burlaga
K. W. Behannon
NASA/Goddard Space Flight Center
Laboratory for Extraterrestrial Physics
Greenbelt, MD 20771

S. F. Hansen
G. W. Pneuman
High Altitude Observatory
National Center for Atmospheric Research
Boulder, CO 80307

W. C. Feldman
Los Alamos Scientific Laboratory
Los Alamos, NM 87544

ABSTRACT

We examined the sources of magnetic fields in recurrent streams observed by the IMP-8 and HEOS spacecraft at 1 AU and by Mariner 10 en route to Mercury between October 31, 1973 and February 9, 1974, during CR 1607 to 1610. Most fields and plasmas at 1 AU were related to coronal holes, and the magnetic field lines were open in those holes. However, some of the magnetic fields and plasmas at 1 AU were related to open field line regions on the sun which were not associated with known coronal holes, indicating that open field lines are more basic than coronal holes as sources of the solar wind. Magnetic field intensities in five equatorial coronal holes, estimated by projecting the measured interplanetary magnetic fields back to the sun using the principle of flux conservation, ranged from 2G to 18G with an average 9G. Average measured photospheric magnetic fields along the footprints of the corresponding unipolar fields on circular equatorial arcs at 2.5 $R_\odot$ had a similar range and average, but in two cases the intensities were approximately three times higher than the projected intensities. The coronal footprints of the sector boundaries on the source surface at 2.5 $R_\odot$, determined by a potential field extrapolation of the measured photospheric fields, meandered between -45° and $+45^\circ$ latitude, and their inclination with respect to the solar equator ranged from near zero degrees at some longitudes to near ninety degrees at others. It is possible that sector boundaries are related to convergence surfaces of the flow near the sun. The high densities observed near sector boundaries between streams might be due in part to the convergence of flows from adjacent coronal holes.

1. INTRODUCTION

For more than fifty years, various investigators have attempted to determine the sources of recurrent interplanetary streams (e.g., see Maunder, 1905; Chapman and Bartels, 1940; Roelof, 1974; Gulbrandson, 1975, and Burlaga and Lepping, 1977). Originally, the issue was whether the sources are solar active regions or some invisible regions called M-regions. Billings and Roberts (1964) suggested that the sources are regions of open magnetic field lines, i.e., photospheric magnetic field lines which extend far from the sun. Recently, it has been argued that the sources are coronal holes (Pneuman, 1973; Noci, 1973; Krieger et al., 1973; Neupert and Pizzo, 1974, Nolte et al., 1976; Sheeley et al., 1976).

Since the interplanetary magnetic field is "frozen" to the plasma, the source of the magnetic field must be essentially the same as the source of plasma. The continuity of field lines implies that the magnetic field lines must be open at the source of a staticnary stream. In particular, if the source of a recurrent stream is a coronal hole, the field lines in the hole must be open. In Sections 2 and 3, we present evidence that this is the case. One problem that remains is to determine whether or not there are open field line source regions which are not associated with coronal holes. This is discussed in Section 3. Another problem of importance is to determine the magnetic field intensity in the source regions, and this is the subject of Section 4.

A related problem that has been a subject of debate is the origin of the sector pattern in the solar wind (i.e., the pattern of the polarity of the interplanetary magnetic field). Does it originate near the ecliptic or at high latitudes? Does it come from isolated nozzles or

from the entire solar surface? What is the character of interplanetary sector boundaries near the solar surface? Does the solar footprint of the surface that forms the boundary between sectors have a high or a low inclination to the equator near the equatorial plane? These questions are addressed in Section 5.

This paper uses observations of interplanetary streams, the interplanetary magnetic field, and coronal holes, together with extrapolations of the photospheric magnetic field, in an attempt to solve the problems discussed above. The data are from November 3, 1973 to February 1, 1974, when the spacecraft IMP-8, HEOS, and Mariner 10 were monitoring the interplanetary medium and Skylab was monitoring the electromagnetic radiation from the solar disk at various wavelengths.

2. RELATIONS BETWEEN INTERPLANETARY STREAMS, THE INTERPLANETARY MAGNETIC FIELD, CORONAL HOLES, AND CORONAL MAGNETIC FIELDS

Figure 1 shows measurements of the interplanetary speed (V), magnetic intensity (B), and magnetic field polarity (+ away from the sun) for three consecutive streams. The speed measurements (3-hour averages) are from the LASL plasma detectors on IMP-7 and IMP-8, which are in orbit around the earth; the magnetic field measurements (hour averages) are from the GSFC magnetometer on IMP-8 and from the magnetometer of Hedgecock on the HEOS 1 and 2 spacecraft, also in earth orbit. The stream marked "2" has the typical form for a corotating stream at 1 AU (e.g., see Hundhausen, 1972). Stream 1 has a similar speed profile, but a very small amplitude. Stream 7 has an unusual, symmetric profile and an intermediate amplitude. The magnetic field intensity is enhanced in the region where V is increasing in each of the streams, as expected from earlier observations (see Hundhausen, 1972) and from kinematics (e.g., see Burlaga and Barouch, 1975 and references therein). The magnetic field in each stream is predominantly of one polarity, and the polarity changes abruptly where the speed is low between stream 2 and stream 1, as expected from past observations (see Hundhausen, 1972).

At the bottom of Figure 1 is a map of coronal holes, determined from X-ray observations by the AS&E group (Nolte et al., 1976). Also shown are the dominant polarities of the photospheric magnetic field in the areas of coronal holes, based on charts compiled by P. McIntosh of NOAA. Note that we do not follow the usual convention in plotting time in the coronal hole maps in Figure 1; the time of central meridian passage (CMP) runs from left to right, making the coronal hole plots compatible with the plots of interplanetary data.

There is an obvious correspondence between the streams and coronal holes in Figure 1. The streams reach 1 AU approximately 3 days after central meridian passage of the corresponding coronal holes. The magnetic polarity of each stream agrees with the polarity in the corresponding coronal hole. This association was first made by Krieger et al. (1973) for these streams. Our data are more complete than those used by Krieger et al. and others, and we do not attempt to project the streams back to the sun, but otherwise, for this rotation, there is no basic difference between our associations and those made earlier (see Nolte et al., 1976). Note that the large stream (2) is associated with a large equatorial coronal hole, the small stream (1) is associated with a small coronal hole near the equator, and the odd-shaped stream (7) is most likely from an extension of a polar hole which comes no closer than 40° to the equator.

Now let us examine how the features discussed above are related to the coronal magnetic fields. These fields were determined as follows. It was assumed that the magnetic field between the photosphere and a spherical source surface at $2.5\,R_{\odot}$ is a potential field, which is determined by a solution of Laplace's equation. For the inner boundary condition, we used photospheric magnetic field measurements from the Kitt Peak Observatory. The outer boundary condition was specified by requiring that the field is radial everywhere on the source surface. The field between these two boundaries was computed by solving Laplace's equation using the numerical technique of Adams and Pneuman (1976). (An equivalent, but different, method of solving Laplace's equation was introduced by Altschuler and Newkirk (1969) and developed by Altschuler et al. (1976).) Only two aspects of these solutions concern us here: 1) the

field intensity on the source surface, and 2) the photospheric "footprints" of the open field lines on the source surface.

Figure 2a shows contours of equal magnetic field intensity on a spherical, sun-centered surface at 1.8 $R_\odot$, computed as discussed above, for part of Carrington Rotation (CR) 1607. Longitude runs from right to left, time of CMP from left to right. There are two maxima of $|\underset{\sim}{B}|$ in the equatorial region, one of positive polarity (solid lines) and the other of negative polarity (dashed lines). The field intensity also increases to a maximum in each polar region. A neutral line (heavy solid curve) separates regions of positive and negative polarity. This line is equivalent to the coronal sector boundary at this height. This neutral line is redrawn in Figure 2b. It intersects the solar equator on November 8, with negative fields before November 8 and positive fields after that date. The magnetic field measurements at 1 AU (Figure 1) show a discontinuous passage from a negative sector to a positive sector on November 13 in qualitative agreement with Figure 2. The mean transit speed of the plasma carrying the neutral line from the sun to the earth was 350 km/sec, in good agreement with the observed speed of the plasma at the time of the sector crossing.

In Figure 2a there is a saddle point between each equatorial maximum in B and the polar maximum of the same polarity; these saddle points are marked by "X's" in Figure 2a. One can construct a curve which passes through the saddle point, which is everywhere normal to equi-intensity contours, and which terminates on the neutral line, as shown by the heavy dashed curves in Figure 2a. Let us call this the saddle line. Figure 2b shows the neutral line and the two saddle lines obtained from

Figure 2a. The physical significance of saddle lines will be discussed later.

The shaded areas in Figure 2b are the photospheric footprints of the "open" magnetic field lines which were computed for the interval that we have been discussing. The sources of the negative polarity fields are shown by the cross-hatched areas, and the sources of the positive polarity fields are shown by the dark areas. Comparing the field line "footprints" in Figure 2b with coronal holes in Figure 1, one finds basically the same patterns in each figure. There is a source of negative open field lines in the south polar regions of Figure 2b which corresponds to the negative southern polar coronal hole in Figure 1, and there are sources of negative open field lines in the equatorial region in Figure 2b which correspond to the negative equatorial hole in Figure 1. Similarly, there is a good correspondence between the sources of positive open field lines in Figure 2b and the coronal holes with positive polarity in Figure 1. Thus, in this case the coronal holes, which are the sources of the interplanetary streams and magnetic fields, are also regions of open magnetic field lines, consistent with the Billings-Roberts hypothesis. A similar association between open field lines near the sun and coronal holes related to interplanetary streams has also been demonstrated by Levine et al. (1977).

3. PLASMA AND MAGNETIC FIELDS FROM OPEN FIELD LINE REGIONS WHICH ARE NOT RELATED TO CORONAL HOLES

Figure 3 shows the interplanetary plasma and magnetic fields and the coronal holes for CR 1608. A combination of a soft X-ray map (Nolte et al., 1976) and a HeII 304 Å map (Bohlin and Rubenstein, 1975), prepared by McIntosh for the Skylab Workshop was used. In Figure 3 and in the Figures which follow, again one can readily associate streams with coronal holes, as shown by the numbering of streams and holes in Figure 3. In general, one finds the expected correspondence between the polarity of magnetic fields in the streams and the polarity of magnetic fields in the coronal holes, but there are three anomalies: 1) there is not just one polarity change between stream 6 and stream 4, 2) similarly, there is not just one polarity change between stream 4 and stream 2, and 3) there is a region of positive polarity in the midst of stream 2, which was associated with a coronal hole of negative polarity. The first two of these effects are related to the problem of sector boundary structure, which will be discussed in a separate paper. The third effect is more directly related to the problem of sources, and can be understood by considering the coronal magnetic field structure shown in Figure 4.

Figure 4b shows the photospheric regions of field lines which are open at 2.5 $R_\odot$ and the corresponding saddle lines for CR 1608. Note that for each coronal hole in Figure 3 there is a corresponding region of open field lines in Figure 4b. However, there is a region of computed open field lines (marked by the question mark in Figure 4) which is not associated with a coronal hole. The field lines in this region have positive polarity, and the region passed central meridan on December 6.

Assuming that the region was a source of interplanetary plasma with a constant speed of 500 km/sec, one would expect to observe magnetic fields of positive polarity in a plasma moving with 500 km/sec at 1 AU on December 9, consistent with the observations in Figure 3. In other words, the anomalous positive polarity magnetic fields in stream 2 on CR 1608 can be attributed to a solar region where the magnetic field lines are open but where there is no observed coronal hole.

The above result is significant, for it suggests that open field lines are more basic for producing interplanetary plasma and magnetic fields than coronal holes. It is thus important to show that it is not simply an isolated result which might be illusory.

Figure 5 shows interplanetary plasma and magnetic field data together with coronal hole (CH) data for CR 1609. One can associate streams 7, 4, and 2* with coronal holes as indicated by the numbering in Figure 5. This correspondence has been made previously by Nolte et al. (1976). Figure 4c shows that the magnetic field lines are open in CH 7, 4 and 2*. However, this association does not explain the source of the negative polarity magnetic fields which were observed in the quiet wind between streams 7 and 4, and it implies that plasma from CH 2* spreads out over a very large range of longitude, $> 100^{\circ}$. The computed solar magnetic field data in Figure 4c provides a possible answer to these difficulties. Figure 4c shows a source of open field lines with negative polarity which could account for the plasma and magnetic fields observed on December 17 and 18 at 1 AU; this source is not associated with an observed coronal hole. There is also a source of open field lines with negative polarity, marked 2** in Figure 4c, which is not associated with a coronal hole, but

which might be the source of a stream which is contiguous with the fastest plasma in stream 2*; in other words, the long complex stream marked 2* in Figure 5 can be regarded as two successive streams, one of which is associated with CH 2*, the other with the open field line region marked 2** in Figure 4c. Note that there was an open field line region of positive polarity (marked "?" in Figure 4c) which was not associated with a coronal hole (see Figure 5); positive polarity fields from this region were not seen at 1 AU, perhaps because the source was south of the equator.

Finally, consider CR 1610. The interplanetary data and the coronal holes are shown in Figure 6. Streams 4 and 2* can be associated with CH 4 and CH 2*, and Figure 4d shows that there are open field line regions with the correct polarity associated with these coronal holes. One might be inclined to associate the stream on January 10 in Figure 6 with CH 7, but CH 7 has the wrong polarity. Figure 4d shows that the stream is related to an open field line region of the right polarity, but note that this region is not associated with an observed coronal hole in Figure 6. The high speed plasma in stream 2* on CR 1610 is clearly associated with an extension of the south polar hole. Figure 4d suggests that the slow plasma observed at 1 AU on February 9 was due to a region at 15° Carrington longitude, which passed central meridian on February 1 and 2. No positive polarity fields were observed corresponding to the open field line region in the southern hemisphere at 55° Carrington longitude.

All of the "anomalous" features from CR's 1608-1610, i.e., those shown to be related to open field line regions without coronal holes, were observed by Mariner 10 as well as by IMP-8 and/or HEOS at 1 AU (see

data plots in Behannon and Ottens, 1976). The radial distance separation between Mariner 10 and Earth increased to approximately 0.2 AU during this period, while the angular separation was $< 10^{o}$ in solar longitude and $< 5^{o}$ in latitude. The correlative data support the interpretation that these interplanetary features were corotating with the sun.

In summary, the data for CR 1607 - CR 1610 show that some plasma and magnetic fields originate in open field line regions that are not related to coronal holes, i.e., coronal holes are sufficient but not necessary sources of plasma and fields. Nevertheless, most of the plasma and magnetic fields that we considered were related to coronal holes in which the magnetic field lines were open. It is beyond the scope of this paper to consider the conditions under which coronal holes develop within open field regions. Such conditions are as yet not well understood, although the rate of field line convergence over a region may be a major factor (Krieger, private communication; Levine et al., 1977). The size of the open field region may also play a role. Figures 3 through 6 support the view that higher speed streams of generally larger dimension come from coronal holes, and that bodies of plasma of smaller extent but unique magnetic polarity, such as observed during this period, originate in the usually smaller open field regions in which no coronal holes have been identified.

4. MAGNETIC FIELD INTENSITIES IN INTERPLANETARY STREAMS AND IN CORONAL HOLES

The magnetic fields near the sun and near 1 AU are related by the condition that magnetic flux is conserved. Thus, the magnetic flux, Φ_h, in a coronal hole with area A_h, is equal to the magnetic flux in a stream at 1 AU, Φ_1 (the subscript h and 1 refer to the coronal hole at 1 $R_\odot$ and to 1 AU, respectively):

$$\Phi_h \equiv \int_{A_h} \underset{\sim}{B}_h \cdot \hat{n} dA_h = \int_{A_1} \underset{\sim}{B}_1 \cdot \hat{n} dA_1 \equiv \Phi_1 , \qquad (1)$$

where $\underset{\sim}{B}_h$ is the magnetic field in a coronal hole, B_1 is the field in the interplanetary medium, and $\hat{n}$ is a unit vector normal to the surface. If the stream comes from a region of open magnetic field lines with no associated hole, then Φ_h is the integral over the area defined by the footprints of the open field lines. Equation (1) assumes, of course, that all of the material in a given stream comes from a single source.

Although the interplanetary magnetic field is measured directly and very accurately, there are several difficulties in determining the magnetic flux in a stream at 1 AU: 1) one must determine the boundaries of the stream associated with a given source; 2) one measures $\underset{\sim}{B}$ only on a curve near the ecliptic plane (the arc of a circle, if measurements are made near earth), so the cross-sectional area of the stream, A_1, is undetermined; 3) the streams are not strictly unipolar, and it is not possible with one spacecraft to determine whether the non-dominant polarities are due to filamentary structures of that polarity which extend to the source, or whether they are due to loops and/or "bottles".

We assume that a sector boundary is a stream boundary. If a sector boundary was not distinct (multiple crossings, mixed polarities, etc.),

we eliminated the ambiguous region and took the beginning or end of the unipolar region as the boundaries and weighted the integrals appropriately. If there was no sector boundary (no polarity change), we assumed that the boundary occurred where the speed was minimum and where the magnetic field intensity just began to rise.

Since the cross sectional area of a stream at 1 AU is unknown, we consider only the incremental flux within the latitude interval $\Delta\theta$, i.e.,

$$\Delta \Phi_1 = \int B_{1x} (r_1 \Delta\theta_1) \, dl_1 , \tag{2}$$

$dl_1 = r_1 d\varphi$ is an element of length of a sun-centered circle with radius 1 AU and B_{1x} is the radial component of the interplanetary field. For a corotating stream, this can be rewritten

$$\Delta \Phi_1 = r_1^2 \Delta\theta_1 \int B_{1x} \, d\varphi = r_1^2 \Delta\theta_1 \Delta\alpha_1 < B_{1x} > . \tag{3}$$

Here $\Delta\alpha_1 = \Omega_s \Delta t$ is the time interval between the two boundaries of the stream, Ω_s is the angular speed of the sun, and $< B_{1x} >$ is the average of B_{1x} over the time interval $\frac{\Delta\alpha_1}{\Omega_s}$. The corresponding magnetic flux in the coronal source is

$$\Delta \Phi_h = r_h^2 \Delta\theta_h \Delta\alpha_h < B_{hx} > . \tag{4}$$

We take $\Delta\alpha_h$ to be the extreme longitudinal limits of the hole, determined from direct measurements of coronal holes. This gives a lower limit on $< B_{hx} >$ for a near-equatorial coronal hole. Equation 1 then gives

$$< B_{hx} > = \left(\frac{r_1}{r_h} \right)^2 F < B_{1x} > , \tag{5}$$

where

$$F \equiv \left(\frac{\Delta\alpha_1}{\Delta\alpha_h}\right)\left(\frac{\delta\theta_1}{\delta\theta_h}\right). \tag{6}$$

Since the axis of a flux tube at 1 AU is 45° from the radial direction, the cross-sectional width of a flux tube at 1 AU is $(r_1\Delta\alpha)$ cos 45°. The longitudinal expansion factor is thus $(r_1\Delta\alpha_1 \cos 45^\circ)/(r_h\Delta\alpha_h)$. The factor $(r_1\delta\theta_1)/(r_h\delta\theta_h)$ measures the latitudinal expansion of the flux-tube; it is generally not known. If the expansion is the same in latitude as it is in longitude, then $\delta\theta_1/\delta\theta_h = (\Delta\alpha_1 \cos 45^\circ)/\Delta\alpha_h$ and substitution into (6) gives

$$F = \left(\frac{\Delta\alpha_1}{\Delta\alpha_h}\right)^2 \cos 45^\circ. \tag{7}$$

The boundaries of the streams that we chose for flux studies are listed for IMP-8/HEOS in Table 1 and shown in Figures 1-4. Similar boundaries were chosen from Mariner 10 data. For Mariner 10, the cosine factor in F was determined for each stream period from the average observed magnetic field spiral angle for that period.

The streams are not strictly unipolar. There are 1 to 4 hour intervals of "foreign" polarity distributed randomly throughout the streams. Table 2 shows that the percentage of dominant polarity ranges from 72% to 94%. Thus, one must consider what average is meant by $< B_{hx} >$ in Equation (5). Three possibilities must be considered: 1) some of the "foreign" polarity is due to sources other than the primary source (e.g., coronal hole) of a stream; 2) the source itself is not unipolar, so that filaments of field with the foreign polarity are immersed in the primary flow, and extend from the source to 1 AU; and 3) source is unipolar but "loops" develop in the solar wind near 1 AU such that part of a filamentary flux tube might be pointing

sunward while another part points anti-sunward. We have already discussed the first point in Section 5. Since we were not able to distinguish between loops and filamentary structures, we shall consider both possibilities. If the foreign polarity is due to such filaments, then strictly speaking one should use $\langle|B_{1x}|\rangle$ in Equation (5). If it is due to loops, then one should average over positive and negative polarity, as implied by $\langle B_{1x}\rangle$. There is also a question of what is meant by $\langle B_{hx}\rangle$. It seems that the photospheric measurements average over positive and negative fields so that one should probably compare it with $\langle B_{1x}\rangle$ rather than $\langle|B_{1x}|\rangle$. Table 2 shows $\langle B_{1x}\rangle$ and $\langle|B_{1x}|\rangle$ for several streams observed by IMP-8/HEOS. $\langle B_{1x}\rangle$ ranges from 1.7γ to 3.8γ, with a median 3.0γ. $\langle|B_{1x}|\rangle$ is somewhat higher, ranging from 2.9γ to 4.5γ, with a meridan of $\approx$ 3.8γ. Table 3 shows similar data from Mariner 10 observations. In addition, it includes the average heliocentric distance of Mariner 10 during each of the stream periods. The results are seen to be similar to those from the observations at 1 AU, although generally higher. Tables 2 and 3 also show the average B_z (normal component) values that were measured in each case.

The magnetic field intensity in each source (coronal hole) can now be estimated from Equation (5) using the data in Tables 1 and 2 from IMP-8/HEOS and equivalent data for Mariner 10. We assume that the expansion of the flow from the holes is the same in latitude and longitude. Since there are at least two possible averages for B_{1x}, ($\langle B_{1x}\rangle$ and $\langle|B_{1x}|\rangle$), there are two possible estimates for B_h. Table 4 shows $\langle B_{hx}\rangle$ obtained from the IMP/HEOS projection and from the Mariner 10 projection. This gives a lower limit for $\langle B_h\rangle$, but it should be comparable to the measured photospheric field, which also averages over

small-scale structure. Table 4 shows that $< |B_{hx}| >$ is 2% to 60% larger than $< B_{hx} >$, and gives an upper limit on B_h. It should not be compared with the measured photospheric fields, however.

The errors of our estimates of $< B_{hx} >$ are the result of uncertainties in the interplanetary measurements of $\underset{\sim}{B}$, the non-uniformities in the interplanetary field, and the projection factor F in (5). The uncertainties due to the interplanetary measurements themselves are negligible. The uncertainties due to non-uniformities in the interplanetary magnetic field can be estimated from the difference between the IMP/HEOS and Mariner 10 projections, which range from 6% to 25%. The greatest uncertainty comes from the expansion factor F in (6), particularly the latitudinal expansion factor $\delta\theta_l/\delta\theta_h$. We have assumed that the expansion in latitude is the same as that in longitude, which is reasonable for the particular near-equatorial holes that we have considered, but the uncertainties could be 50% or more.

We have determined the "measured" photospheric fields which are to be compared with our estimates in Table 4 as follows. The field at 2.5 $R_\odot$ was computed using the potential field extrapolation as described in Section 2; at 2.5 $R_\odot$, the longitudinal extent in the equatorial plane of the single polarity region corresponding to each coronal hole was determined; the field lines on each of these circular arcs were traced back to the solar surface; and the average B_{hx} along those footprints was computed. Generally, the footprints had a smaller longitudinal extent than the coronal holes, and it depends on the location of the source surface Nevertheless, this method should give the average magnetic field intensity of open-field lines in coronal holes to within a factor of 1.5. The

resulting values for the "observed" coronal hole magnetic field intensities along the footprints are shown in the last column of Table 4, next to the averages of the IMP-HEOS and Mariner 10 estimates of B_h. There is good agreement between the projected and "observed" field intensities in CH 4. For CH 2 on CR 1607 the "observed" intensity is $\approx$ 3.3 times the projected intensity, and for CH 1 on CR 1607 the "observed" intensity is $\approx$ 2.7 times the projected intensity. The fields measured by IMP/HEOS and Mariner 10 for CH 1 and 2 are not significantly lower than those for CH 4, so the discrepancy is probably due to an error in our estimate of F and/or an error in the "observed" intensity along the computed footprints. In any case, the collective results in Table 4 show that the intensity of "open" magnetic fields in coronal holes can range from a few G to $\approx$ 20 G, the average being $\approx$ 10 G for the five holes that we considered.

Using a potential field method, Levine et al. (1977) have computed the fields at 1 AU from measured photospheric field. With a source surface at 2.6 $R_\odot$, they find an average radial field component at 1 AU of 0.7×10^{-5} G, for equatorial open-field lines. This is 5 times smaller than the observed value, and it implies that the computed intensities at the source surface are too small by a factor of $\approx$ 5. The intensities which we computed at 2.5 $R_\odot$ are essentially the same as those which Levine et al., computed at that distance. However, our estimates of the coronal hole fields do not depend on these computed intensities. We used the potential field method only to identify open-field lines. The coronal hole intensities given in Table 4 are photospheric measurements along points at which the field lines are open. It would seem that the potential

field method identifies some but not all open-field lines and that it does not accurately extrapolate measured intensities from 1 $R_\odot$ to 2.6 $R_\odot$.

5. SECTOR BOUNDARIES

We have already noted that the heavy curves in Figures 2 and 4 are the neutral lines (sector boundaries) at 2.5 $R_\odot$, i.e., at this line $B_r = 0$ and the polarity of the field changes. The figures show two important features of the sector boundaries during this timer period: 1) They are confined to within $\pm 45^\circ$ of the equator. 2) Their inclination with respect to the equator ranges from near zero degrees to near 90° and varies in an irregular manner. The two features just mentioned are not sensitive to our method of determining the null lines.

The latitudinal extent of sector boundaries has recently been a subject of debate. Rosenberg and Coleman (1969), Schultz (1973), and Hansen et al. (1974) suggested that the boundaries lie near the ecliptic plane, corresponding to a large-scale, north-south dipole field of the sun. On the other hand, Wilcox and Svalgaard (1974) suggested that the boundaries can extend to high latitudes. Our results indicate that the truth was between these two extremes in the period that we considered; the boundaries meandered between -45° and $+45^\circ$ latitude. This consistent with the model of Svalgaard et al. (1974, 1975). Note that the open field line regions marked by a question mark in Figure 4 introduces a complication not considered by the previous authors: there can be more than one closed neutral line. In particular, the regions marked by "?" in Figure 4 introduce polarity reversals in the field at 1 AU and would contribute to the "dominant polarity effect" discussed by Rosenberg and Coleman (1969). The complications introduced by these regions are not serious in the interval that we are considering, but generally one must take care to avoid possible confusion with the effects of a single, global current sheet.

The inclination of sector boundaries with respect to the equator is small near the sun in the model of Schulz (1973) and Hansen et al. (1974), but large in the picture of Svalgaard et al. (1974). Our results indicate that it is small in some regions near the sun and large in others, depending on the location and "strength" of the sources of open field lines. This is illustrated in Figure 7. If there are just two sources, one near the sun's north pole and the other near the south pole, then the sector boundary lies in the equatorial region (Figure 7a, c). Two isolated polar sources and one equatorial source imply a sector boundary which is in the equatorial plane at longitudes far from the equatorial source and which has an intermediate inclination at longitudes near the source (Figure 7b). Finally, two isolated polar sources and two neighboring equatorial sources imply a large inclination of the sector boundaries between the equatorial sources and a small inclination far from them (Figure 7d). In summary, the shape of the sector boundaries depends very much on the number and relative positions of the coronal holes and open field line regions.

6. CORONAL FLOWS

It is inferred that the solar wind comes from isolated regions on the sun, and it is observed that there is no vacuum in the solar wind. Thus, there must be a diverging flow from each source in the corona such as to fill the voids. Since the magnetic pressure exceeds the thermal pressure, the flow is strongly channeled along the field lines, as described in the model of Pneuman (1973), Pneuman and Kopp (1970, 1971) and by Parker (1963) for an isolated source.

In general, there are two or more sources on the sun at any instant, and flow from adjacent sources must converge toward a surface which extends away from the sun. In other words, one can speak of convergence surfaces of the flow in the corona. The intersection of such a surface with a sun-centered sphere of radius $\approx$ 2 to 10 $R_\odot$ is a line, which we call a convergence line. Figure 8 shows convergence lines surrounding the coronal holes on CR 1607. The arrows pointing away from the holes indicate schematically that there is a component of flow parallel to the photospheric surface which causes a divergence of flow from each hole. Consider the flow from CH 2. Plasma with negative polarity magnetic fields moves northward from CH 2 and meets plasma with positive polarity fields flowing southward from the coronal hole in the northern polar region. Similarly, material with negative polarity fields moves from CH 2 toward CH 1 and meets material with positive polarity fields flowing from CH 1. These flows will thus converge toward a surface which runs approximately East-West between the north-polar hole and CH 2 and which runs approximately North-South between CH 2 and CH 1. A projection of the convergence line associated with this surface is shown by the solid curve in Figure 8.

The arrows indicate that flow converges toward the surface associated with this line. As a zeroth approximation, the line was drawn such that it runs approximately midway between adjacent holes. This line separates fields of opposite polarity; hence, we shall call it a negative convergence line. Comparing it with the neutral line in Figure 2, one finds that this negative convergence line corresponds with the coronal "footprint" of a sector boundary. The flows separated by the sector boundary have distinctly different origins.

The southward flow from the equatorial CH 2 converges with the northward flow from the southern polar coronal hole somewhere in the corona. This is indicated by the dashed line drawn midway between CH 2 and the south-polar hole in Figure 8. Since the polarity of the fields near a source surface is the same on both sides of this line, we shall call it a positive convergence line. (Note that the polarity of photospheric fields under the positive convergence line might be variable, but presumably those field lines are closed and do not extend through the corona.) Comparing Figure 8 with Figure 2, one finds that positive convergence lines of the flow correspond to saddle lines in the magnetic field on the source surface. There should be a corresponding boundary separating flows with like polarity in interplanetary space; one obvious candidate is the stream interface (Belcher and Davis, 1971, Burlaga, 1974).

The convergence of flows from adjacent coronal holes would produce an enhancement of density near the convergence line if the flow is not strictly along $\underset{\sim}{B}$ near the sun. This would imply high densities near sector boundaries and interfaces in the low speed regions between streams in the interplanetary medium as is observed (Belcher and Davis, 1971; Neugebauer and Snyder, 1966; Burlaga and Ogilvie, 1970).

7. SUMMARY

We examined the relations between coronal holes, coronal magnetic fields, interplanetary plasma, and interplanetary magnetic fields for four solar rotations, CR 1607 to CR 1610, in the interval October 31, 1973 to February 9, 1974. This was a period near solar minimum, when solar activity was low and the interplanetary medium was dominated by two exceptionally stable streams.

We confirmed the associations between the major streams and coronal holes that were made previously. Assuming potential fields near the sun, we showed that the solar magnetic field lines were open in the neighborhood of the coronal holes. We identified other open magnetic field lines on the sun which were not associated with coronal holes, and we found interplanetary plasma and magnetic fields which were associated with these open lines. In this sense, open field lines are more basic than coronal holes as a source of interplanetary plasma and fields, although most of the plasma in the interval that we considered did come from coronal holes. In particular, the plasma and fields in all the large-scale, high speed streams that were observed were found to originate in coronal holes, in agreement with the results of other investigations. Most of the material was associated with coronal holes and open magnetic field line regions near the solar equator; however, one stream was associated with an extension of the north-polar hole to $\approx 45^{\circ}$ latitude, and there was presumably a latitudinal flow along field lines near the sun which brought the material from 45° to the equatorial plane where it was observed.

We estimated the magnetic field intensity in five equatorial holes by using interplanetary measurements and the conservation of magnetic

flux. The intensity ranged from 2G to 18G with an average of 9G for the fluxes measured at 1 AU. Similar results were obtained for Mariner 10. Measured photospheric magnetic fields along the computed footprints of open magnetic field lines in coronal holes have the same range and average, but in two cases those measured values were three times larger than the projected values.

The potential field solutions give a null line, where the polarity of the magnetic field reverses and the intensity is zero on any spherical surface centered at the sun. This is the intersection of the sector boundary with the surface. In the interval that we considered, this intersection at 1.8 $R_\odot$ meandered approximately midway between coronal holes and was confined to latitudes between -45° and $+45^\circ$. The inclination with respect to the equator ranged from nearly zero degrees to nearly ninety degrees. There are probably some additional detailed distortions between 1.8 $R_\odot$ and 1 AU, but the basic polarity pattern observed at 1 AU is clearly related to the polarity pattern near the sun.

Sector boundaries separate flows from pairs of distinctly different sources with opposite magnetic field polarities. They presumably correspond to convergence surfaces ("negative" convergence surfaces) in the flow in the outer corona. There should be similar convergence surfaces separating flows from sources with the same magnetic polarity ("positive" convergence surfaces). We identify "saddle lines", which were defined by the potential field mapping results, as the intersection of positive convergence surfaces on a spherical surface centered at the sun. There should be a corresponding plasma boundary in interplanetary space. The high densities observed near sector boundaries and interfaces between

streams in the interplanetary medium could be due, at least in part, to the convergence of flows from adjacent coronal holes.

ACKNOWLEDGMENTS

This work originated as a result of our participation in the NASA Skylab Workshop on Coronal Holes, and it was influenced by presentations and discussions at that workshop. The coronal hole maps used in this paper were presented at that meeting. J. Harvey provided the Kitt Peak photospheric magnetic field observations, which were essential to this study. P. McIntosh provided H-alpha synoptic charts, with traces of coronal holes. The plasma data are from the LASL IMP-6 data. Mark Silverstein and Frank Ottens provided programming assistance.

REFERENCES

Adams, J. and G. W. Pneuman, "A new technique for the determination of coronal magnetic fields: A fixed mesh solution to Laplace's equation using line-of-sight boundary conditions", Solar Phys., 46, 185, 1976.

Altschuler, M. D. and G. Newkirk, Jr., "Magnetic fields and the structure of the solar corona, 1, Method of calculating coronal fields", Solar Phys., 9, 131, 1969.

Altschuler, M. D., R. H. Levine, M. Stix, and J. W. Harvey, "High resolution mapping of the magnetic field of the solar corona", Solar Phys., in press, 1976.

Behannon, K. W. and F. W. Ottens, "Mariner 10 interplanetary magnetic field measurements November 1973 - March 1974", NASA/GSFC Tech. Report X-692-76-208, 1976.

Belcher, J. W. and L. Davis, Jr., "Large-amplitude Alfvén waves in the interplanetary medium, 2", J. Geophys. Res., 76, 3534, 1971.

Billings, D. E. and W. O. Roberts, "The origin of M-region geomagnetic storms", Astrophys. Norv. 9, 1947, 1964.

Bohlin, J. D. and D. M. Rubenstein, "Synoptic maps of solar coronal hole boundaries derived from HeII 304 Å spectroheliograms from the manned skylab missions", World Data Center A Report UAG-51, 1975.

Burlaga, L., "Interplanetary stream interfaces", J. Geophys. Re., 79, 3717, 1974.

Burlaga, L. and E. Barouch, "Interplanetary stream magnetism: kinematic effects", Astrophys. J., 203, 257, 1975.

Burlaga, L. F. and R. Lepping, "The causes of recurrent geomagnetic storms", Planet. Space Sci., in press, 1977.

Burlaga, L. F. and K. W. Ogilvie, "Magnetic and thermal pressures in the solar wind", Solar Phys., 15, 61, 1970.

Chapman, S. and J. Bartels, "Geomagnetism", Ch. 12, Oxford University Press, Oxford, 1940.

Gulbrandsen, A., "The solar M-region problem--an old problem now facing its solution?", Planet. Space Sci., 23, 143, 1975.

Hansen, S. F., C. Sawyer, and R. T. Hansen, "K corona and magnetic sector boundaries", Geophys. Res. Ltrs., 1, 13, 1974.

Hundhausen, A. J., "Coronal expansion and solar wind", Springer-Verlag, New York, 1972.

Krieger, A. S., A. F. Timothy, and E. C. Roelof, "A coronal hole and its identification as the source of a high velocity solar wind stream", Solar Phys., 29, 505, 1973.

Levine, R. H., M. D. Altschuler, and J. W. Harvey, "Solar sources of the interplanetary magnetic field and solar wind", J. Geophys. Res., 82, 1061, 1977.

Levine, R. H., M. D. Altschuler, J. W. Harvey, and B. V. Jackson, "Open Magnetic Field Structures on the Sun", Astrophys. J., 1977.

Maunder, E. W., "Magnetic disturbances, 1882 to 1903, as recorded at the Royal Observatory, Greenwich, and their association with sunspots", Monthly Notices Roy. Astron. Soc., London, 65, 2, 1905.

Neugebauer, M. and C. W. Snyder, "Mariner 2 observations of the solar wind 1. Average properties", J. Geophys. Res., 71, 4469, 1966.

Neupert, W. M. and V. Pizzo, "Solar coronal holes as sources of recurrent geomagnetic disturbances", J. Geophys. Res., 79, 3701, 1974.

Noci, G., "Energy budget in coronal holes", Solar Phys., 28, 403, 1973.

Nolte, J. T., A. S. Krieger, A. F. Timothy, R. E. Gold, E. C. Roelof, G. Vaiana, A. J. Lazarus, J. D. Sullivan, and P. S. McIntosh, "Coronal holes as sources of solar wind", Solar Phys., 46, 303, 1976.

Parker, E. N., "Interplanetary Dynamical Processes", Interscience, New York, 1963.

Pneuman, G. W., "The solar wind and the temperature-density structure of the solar corona", Solar Phys. 28, 247, 1973.

Pneuman, G. W. and R. A. Kopp, "Coronal streamers III. Energy transport in streamers and interstreamer regions", Solar Phys. 13, 176, 1970.

Pneuman, G. W. and R. A. Kopp, "Gas-magnetic field interactions in the solar corona", Solar Phys., 18, 258, 1971.

Roelof, E. C., "Coronal structure and the solar wind", in Solar Wind Three, C. T. Russell, p. 98, Inst. of Geophysics and Planetary Physics, UCLA, 1974.

Rosenberg, R. L. and P. J. Coleman, Jr., "Latitude dependence of the dominant polarity of the interplanetary magnetic field", J. Geophys. Res., 74, 5611, 1969.

Schulz, M., "Interplanetary sector structure and the heliomagnetic equator", Astrophys. and Space Sci., 24, 371, 1973.

Sheeley, N. R., Jr., J. W. Harvey, and W. C. Feldman, "Coronal holes, solar wind streams, and recurrent geomagnetic disturbances: 1973-1976", Naval Research Laboratory Technical Report, 1976.

Svalgaard, L., J. M. Wilcox, and T. L. Duvall, "A model combining the polar and sector-structured solar magnetic fields", Solar Phys., 37 157, 1974.

Svalgaard, L., J. M. Wilcox, and P. H. Scherrer, "The sun's magnetic sector structure", Solar Phys., 45, 83, 1975.

Wilcox, J. M. and L. Svalgaard, "Coronal magnetic structure at a solar sector boundary", Solar Phys., 34, 461, 1974.

TABLE 1

INTERPLANETARY DATA

CR	Hole	Stream Start Day	Stream Start Hour	Stream End Day	Stream End Hour	Interval (Hour)	Data Coverage (Hour)
1607	1	316.	6.	319.	12	78	62
1608	4	326.	19.	336.	15	236	180
1609	4	352	3.	360.	20.	209	140
1610	4	13	9.	23	12	243	115
1607	2	307.	0.	316.	6.	222	214

TABLE 2

IMP 8/HEOS INTERPLANETARY STREAM MAGNETIC FIELDS

CH	CR	$B_z(\gamma)$	% Polarity	$< B_{1x} > (\gamma)$	$< \lvert B_{1x} \rvert > (\gamma)$
1	1607	0.03	77	2.7	3.5
4	1608	-0.19	72	1.7	2.9
	1609	0.02	77	3.4	4.5
	1610	-0.53	85	3.8	4.1
2	1607	0.08	94	-3.8	4.1

TABLE 3

MARINER 10 INTERPLANETARY STREAM MAGNETIC FIELDS

CH	CR	$< r >$ (AU)	$B_z(\gamma)$	% Polarity	$< B_x > (\gamma)$	$< \lvert B_x \rvert > (\gamma)$
1	1607	0.99	-0.15	82	3.1	4.2
4	1608	0.97	0.20	84	2.1	3.4
	1609	0.91	0.35	96	5.0	5.1
	1610	0.80	-0.22	86	4.3	4.7
2	1607	0.99	-0.07	89	-3.1	3.4

TABLE 4

CORONAL HOLE MAGNETIC FIELDS ESTIMATED FROM INTERPLANETARY AND SOLAR OBSERVATIONS

CH	CR	F	FROM (IMP/HEOS)	$< B_{hx} >$ FROM (M10)	OPEN SOLAR FIELD
1	1607	1.1	1.4 G	1.8 G	4.3 G
4	1608	14.2	11.1 G	8.6 G	5.6 G
4	1609	6.4	10.0 G	11.5 G	10.0 G
4	1610	10.5	18.4 G	22.2 G	24.0 G
2	1607	3.3	5.9 G	6.6 G	21.0 G

FIGURE CAPTIONS

Figure 1 The top panel shows three interplanetary streams observed at 1 AU, together with the magnetic field intensities and polarities in these streams. The bottom panel shows a map of the coronal holes from which the streams probably originated. The photospheric magnetic field polarities in the coronal holes agree with the polarities in streams at 1 AU.

Figure 2 a) Equi-intensity contours of the magnetic field at 1.8 $R_\odot$, computed from a potential field extrapolation of the measured photospheric magnetic field with a source surface at 2.5 $R_\odot$.
b) Observations of the footprints of open magnetic field lines together with the null line and saddle lines from Figure 2a. Solid areas indicate positive (outward) polarity and diagonal lines indicate negative polarity. Comparison with Figure 1 shows that the locations of open field line regions correspond to positions of the coronal holes.

Figure 3 Observations of the interplanetary streams and magnetic fields at 1 AU and the coronal holes and photospheric polarities under the holes, for CR 1608. There is a general association between the streams and the holes, but the boundaries of stream 4 are not sharp, and there is a flow with positive polarity in stream 2 which is not related to a coronal hole.

Figure 4 Map of the footprints of open magnetic field lines, their polarities, (solid areas have positive polarity), the null lines (solid curves), and the saddle lines (dashed curves) for CR 1607 through CR 1610.

Figure 5 Interplanetary streams and magnetic fields for CR 1609.

Figure 6 Interplanetary streams and magnetic fields for CR 1610.

Figure 7 This illustrates some basic types of arrangements of coronal holes and the shapes of the footprints of the corresponding sector boundaries and saddle surfaces. Inclination and latitudinal extent of the sector boundaries depends on the relative positions of coronal holes.

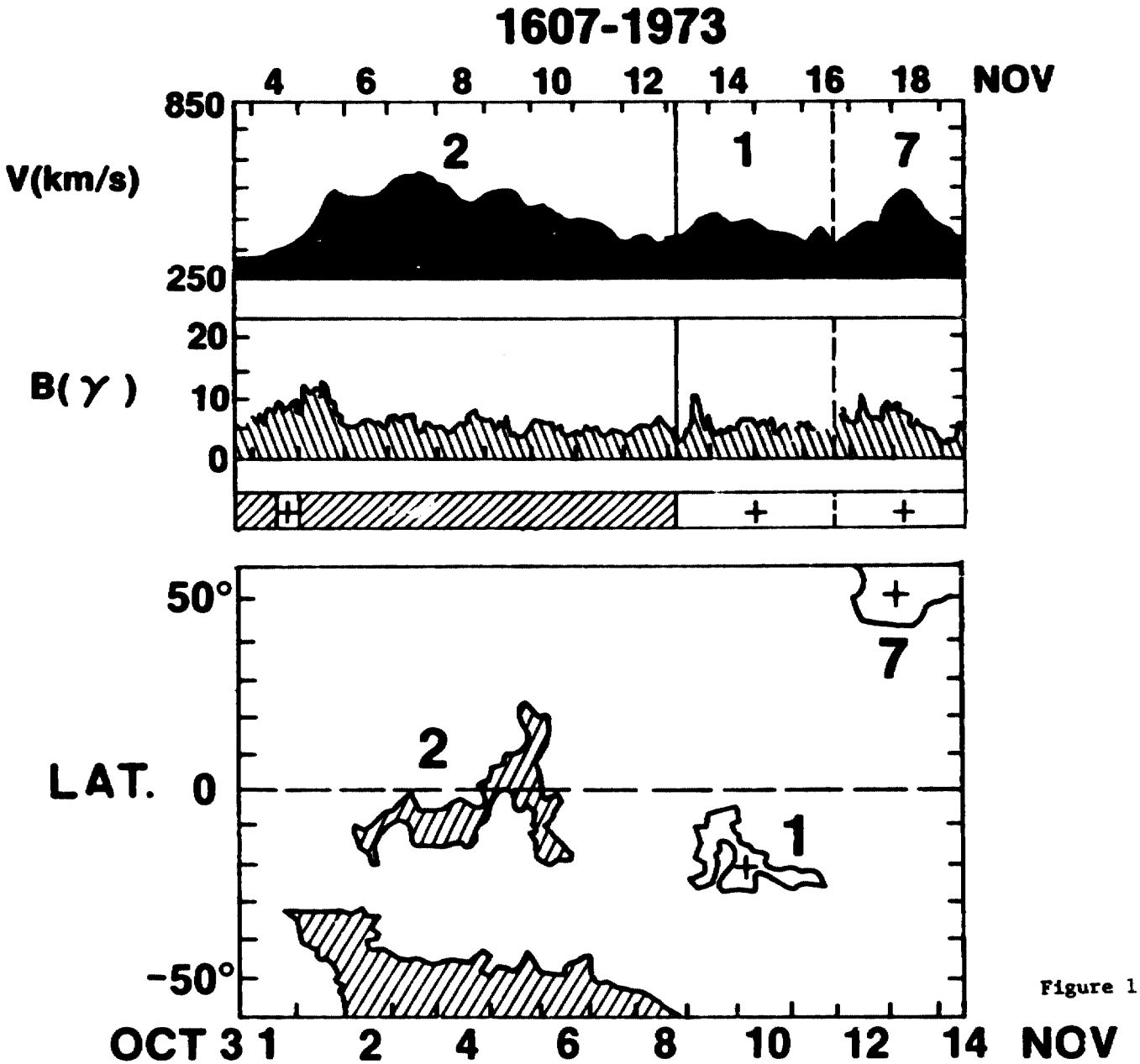
1607-1973
4
6
8
10
12
14
16
18
NOV
850
250
V(km/s)
2
1
7
20
10
0
B(γ)
+
+
+
50°
0
-50°
LAT.
7
2
1
+
+
OCT 3 1
2
4
6
8
10
12
14
NOV

Figure 1

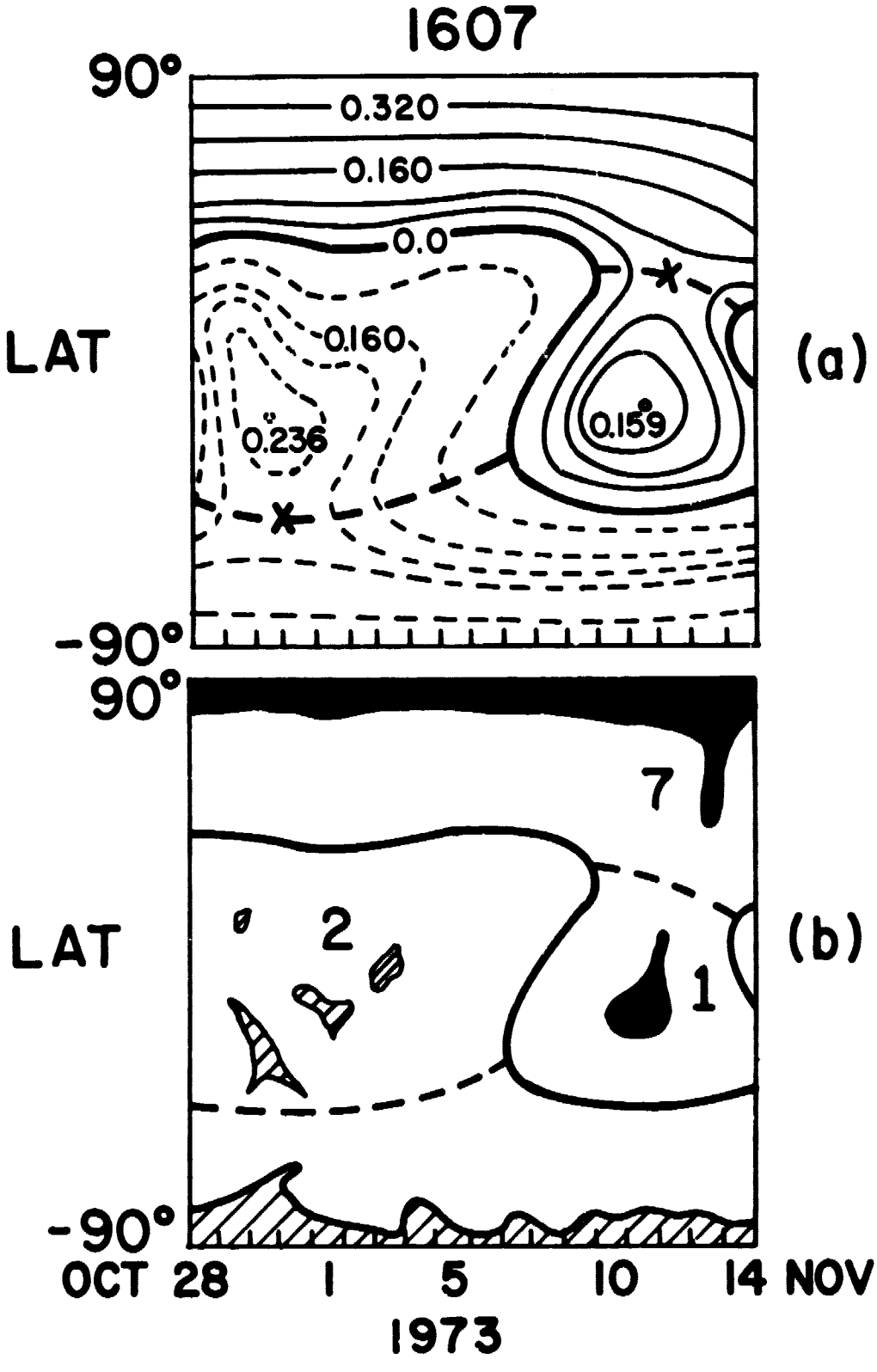
1607
90°
0.320
0.160
0.0
LAT
0.160
(a)
0.236
0.159
-90°
90°
7
LAT
2
1
(b)
-90°
OCT 28
1
5
10
14 NOV
1973

Figure 2

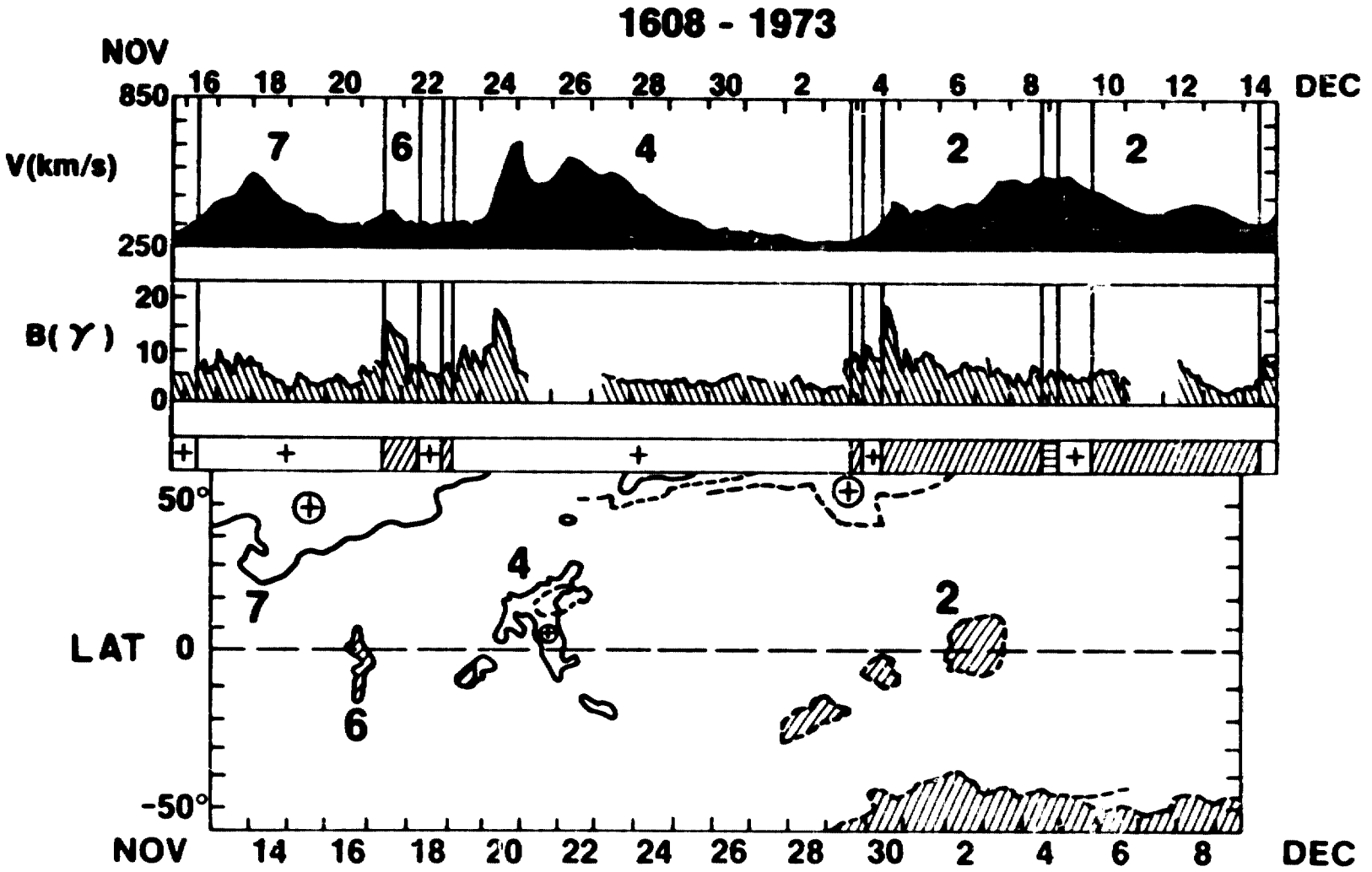
1608 - 1973
NOV
16 18 20 22 24 26 28 30 2 4 6 8 10 12 14 DEC
850
V(km/s)
250
7
6
4
2
2
20
B(γ)
10
0
+
50°
LAT 0
-50°
7
6
4
2
NOV 14 16 18 20 22 24 26 28 30 2 4 6 8 DEC

Figure 3

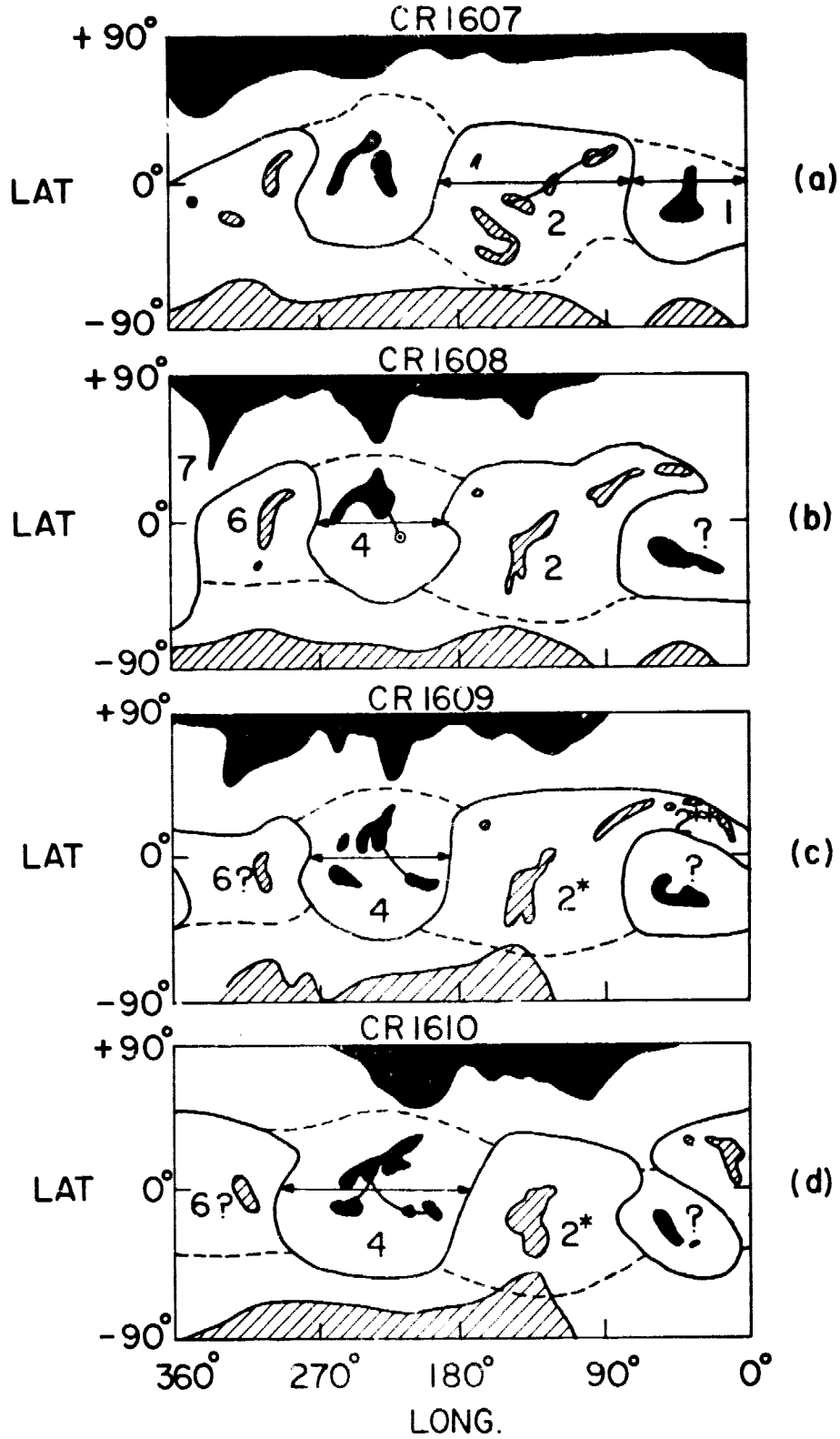
CR1607
+90°
LAT
0°
-90°
2
1
(a)
CR1608
+90°
7
LAT
0°
6
4
2
?
(b)
-90°
CR1609
+90°
LAT
0°
6?
4
2*
?
(c)
-90°
CR1610
+90°
LAT
0°
6?
4
2*
?
(d)
-90°
360°
270°
180°
90°
0°
LONG.

Figure 4

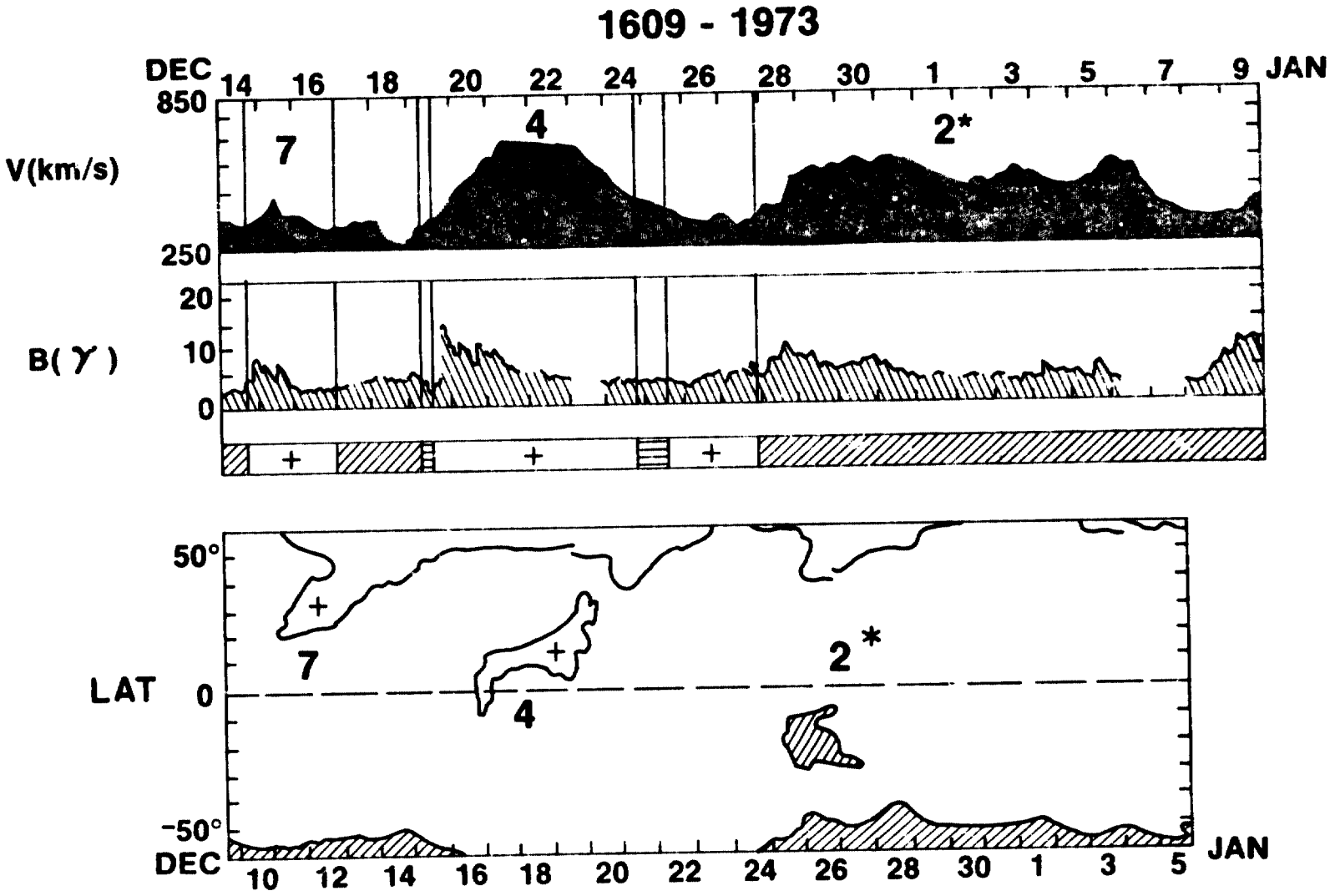
1609 - 1973
DEC
14 16 18 20 22 24 26 28 30 1 3 5 7 9 JAN
850
250
V(km/s)
7
4
2*
20
10
0
B(γ)
+
+
+
50°
0
-50°
LAT
7
4
2*
DEC
10 12 14 16 18 20 22 24 26 28 30 1 3 5
JAN

Figure 5

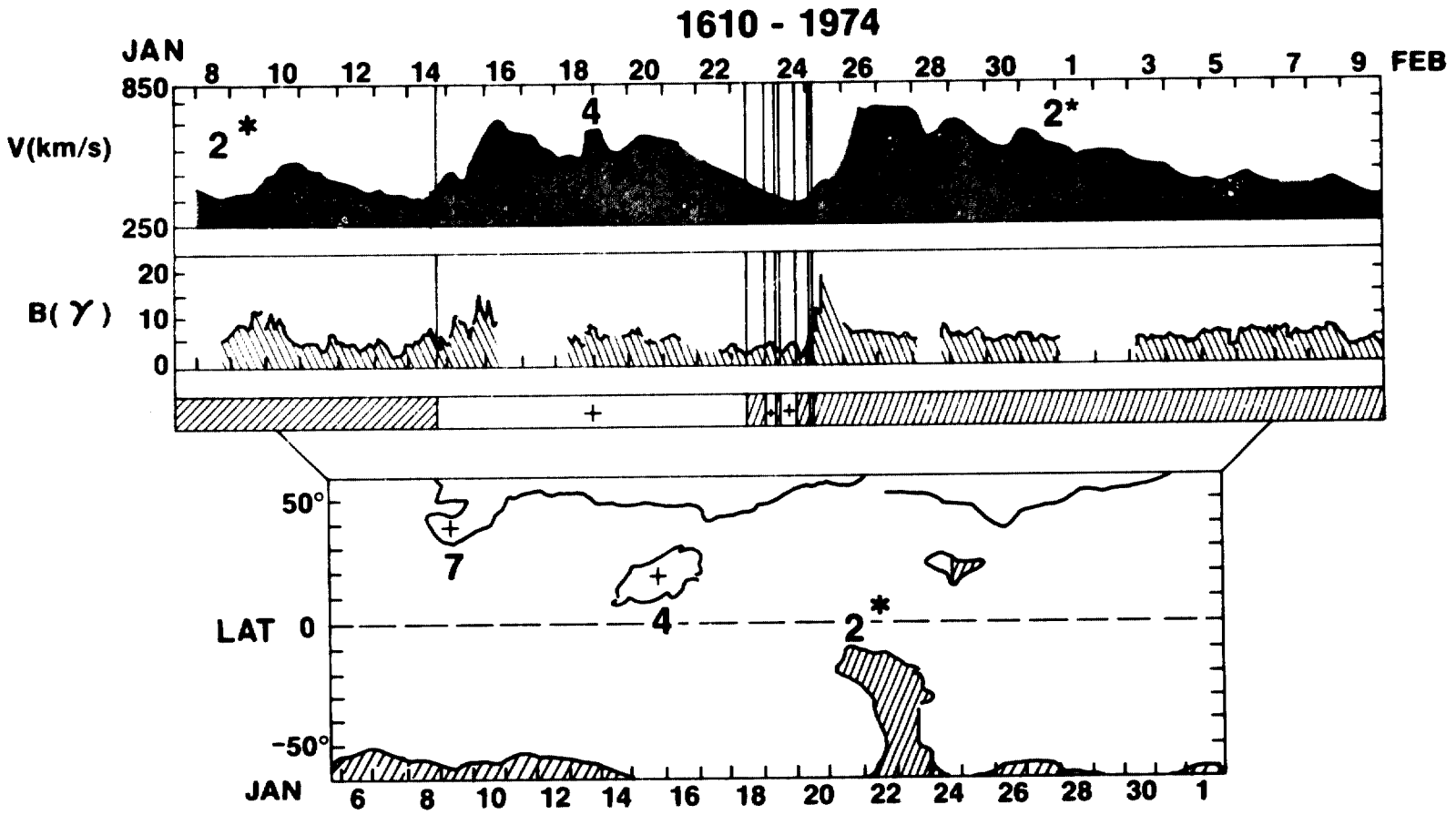
1610 - 1974
JAN
8 10 12 14 16 18 20 22 24 26 28 30 1 3 5 7 9 FEB
850
V(km/s)
250
2*
4
2*
20
B(γ)
10
0
+
+
+
50°
7
LAT 0
4
2*
-50°
JAN
6 8 10 12 14 16 18 20 22 24 26 28 30 1

Figure 6

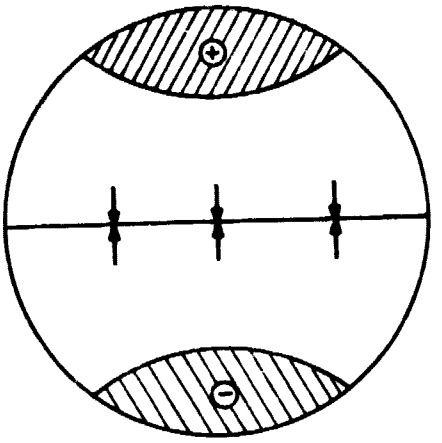

(a)

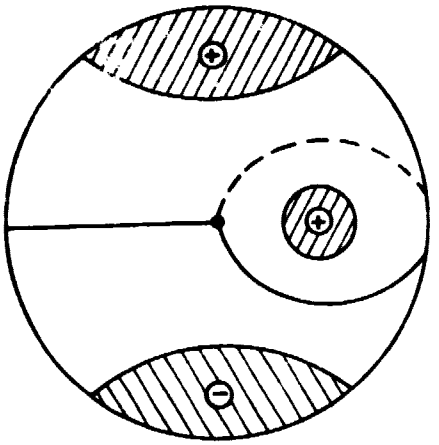

(b)

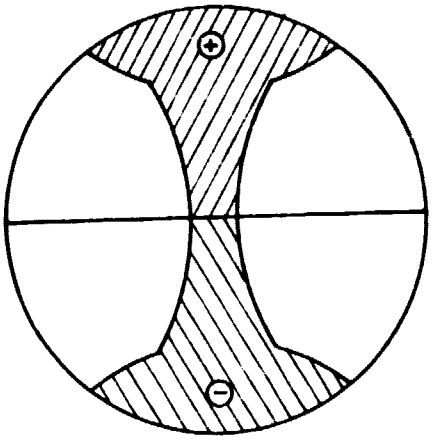

(c)

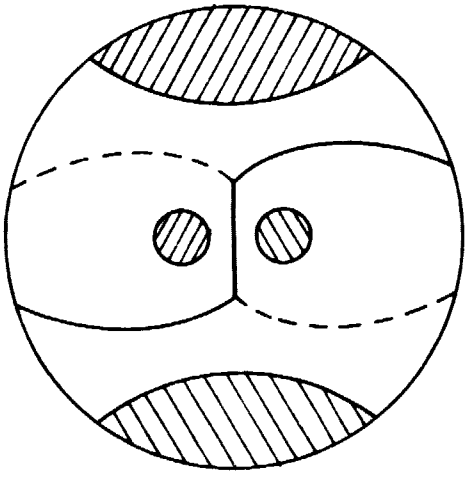

(d)

Figure 7